

# Scalable Support Vector Clustering Using Budget

Tung Pham<sup>a</sup>, Trung Le<sup>b,\*</sup>, Hang Dang<sup>a</sup>

<sup>a</sup>*Faculty of Information Technology, VNUHCM-University of Science, Vietnam*

<sup>b</sup>*Centre for Pattern Recognition and Data Analytics, Deakin University, Australia*

---

## Abstract

Owing to its application in solving the difficult and diverse clustering or outlier detection problem, support-based clustering has recently drawn plenty of attention. Support-based clustering method always undergoes two phases: finding the domain of novelty and performing clustering assignment. To find the domain of novelty, the training time given by the current solvers is typically over-quadratic in the training size, and hence precluding the usage of support-based clustering method for large-scale datasets. In this paper, we propose applying Stochastic Gradient Descent (SGD) framework to the first phase of support-based clustering for finding the domain of novelty and a new strategy to perform the clustering assignment. However, the direct application of SGD to the first phase of support-based clustering is vulnerable to the curse of kernelization, that is, the model size linearly grows up with the data size accumulated overtime. To address this issue, we invoke the budget approach which allows us to restrict the model size to a small budget. Our new strategy for clustering assignment enables a fast computation by means of reducing the task of clustering assignment on the full training set to the same task on a significantly smaller set. We also provide a rigorous theoretical analysis about the convergence rate for the proposed method. Finally, we validate our proposed method on the well-known datasets for clustering to show that the proposed method offers a comparable clustering quality while simultaneously achieving significant speedup in comparison with the baselines.

*Keywords:* Support Vector Clustering, Kernel Method, Stochastic Gradient Descent, Budgeted Stochastic Gradient Descent.

---

## 1. Introduction

Cluster analysis is a fundamental problem in pattern recognition and machine learning which has a wide spectrum of applications in reality. The goal of cluster analysis is to categorize objects into groups or clusters based on pairwise similarities between those objects such that two criteria, homogeneity and

---

\*Corresponding author

*Email address:* [trung.l@deakin.edu.au](mailto:trung.l@deakin.edu.au) (Trung Le)

separation, are achieved [35]. Two challenging tasks in cluster analysis are (1) to deal with complicated data with nested or hierarchy structures inside; and (2) to automatically detect the number of clusters. Recently inspired from the seminal work of [1], support-based clustering has drawn a significant research concern because of its applications in solving the difficult and diverse clustering or outlier detection problem [1, 39, 26, 2, 9, 20, 14]. The support-based clustering methods have two main advantages in comparison to other clustering methods: (1) ability to generate the clustering boundaries with arbitrary shapes and automatically discover the number of clusters; and (2) capability to handle well the outliers.

Support-based clustering methods always undergo two phases. In the first phase (i.e., finding the domain of novelty), an optimal hypersphere [1, 36, 13, 18, 19, 17] or hyperplane [31, 25] is discovered in the feature space. The domain of novelty when mapped back into the input space will become a set of contours tightly enclosing data which can be interpreted as cluster boundaries. However, this set of contours does not point out the assignment of data samples to clusters. Furthermore, the computational complexity of the current solvers [8, 4] to find out the domain of novelty is often over-quadratic [32]. Such a computational complexity renders the application of support-based clustering methods for the real-world datasets impractical. In the second phase (i.e., clustering assignment), based on the geometry information carried in the resultant set of contours obtained from the first phase, data samples are appointed to their clusters. Several existing works have been proposed to improve cluster assignment procedure [39, 26, 2, 20, 9].

Recently, stochastic gradient descent (SGD) frameworks [30, 33, 34, 7] have offered building blocks to develop scalable learning methods for efficiently handling large-scale dataset. SGD-based algorithm has the following advantages: (1) very fast; (2) ability to run in online mode; and (3) economic in memory usage. In this paper, we conjoin the strengths of SGD with support-based clustering. In particular, we propose to use the optimal hyperplane as the domain of novelty. The margin, i.e., the distance from the origin to the optimal hyperplane, is maximized to make the contours enclosing the data as tightly as possible. Subsequently, we employ the SGD framework proposed in [33] to the first phase of support-based clustering to efficiently solve the incurred optimization problem. Unfortunately, this direct employment [27] is vulnerable to the *curse of kernelization* [37] wherein the model size linearly grows up with the data size accumulated over time. To address this issue, we utilize the budget approach [5, 3, 38, 37, 11, 10, 15, 16] to restrict the model size to a budget, and hence keeping the most important data samples whilst partly preserving the information of the less important ones. More specifically, a budget maintenance procedure (e.g., removal, projection, or merging) is invoked to maintain the model size whenever this model size exceeds the budget. Finally, we propose a new strategy for clustering assignment where each data sample in the extended decision boundary has its own trajectory to converge to an equilibrium point and clustering assignment task is then reduced to the same task for those equilibrium points. Our clustering assignment strategy distinguishes from

the existing works of [20, 21, 9, 22] in the way to find the trajectory with a start and the initial set of data samples that need to do a trajectory for finding the corresponding equilibrium point. The experiments established on the real-world datasets show that our proposed method produces the comparable clustering quality with other support-based clustering methods while simultaneously achieving the computational speedup.

To summarize, the contribution of the paper consists of the following points:

- In contrast to the works of [1, 2, 20, 26, 39] which employ a hypersphere to describe the domain of novelty, we propose using a hyperplane to characterize the domain of novelty. This allows us to introduce SGD-based solution for finding the domain of novelty.
- We propose budgeted SGD-based solution for finding the domain of novelty which allows the incurred optimization to be efficiently solved and to be invulnerable to the curse of kernelization. We perform a rigorous convergence analysis for the proposed solution. We note that the works of [1, 2, 20, 26, 39] utilized the Sequential Minimal Optimization based approach [29] to find the domain of novelty wherein the computational complexity is over-quadratic and the memory usage is inefficient since the entire Gram matrix is required to load into the main memory.
- We propose new clustering assignment strategy which can reduce the clustering assignment for  $N$  samples in the entire training set to the same task for  $M$  equilibrium points where  $M$  is usually very small by a wide margin comparing to  $N$ .

The rest of this paper is organized as follows. In Section 2, we recall large margin one-class support vector machine [25, 12]. In Section 3, we introduce the budgeted stochastic gradient approach to solve the optimization problem of large margin one-class support vector machine in its primal form. In Section 4, we present our proposed clustering assignment. Finally, in Section 5, we conduct the extensive experiments and then discuss on the experimental results. In addition, all proofs are given in the appendix section.

## 2. Large margin one-class support vector machine

Given the dataset  $\mathcal{D} = \{x_1, x_2, \dots, x_N\}$ , to define the domain of novelty, we construct an optimal hyperplane that can separate the data samples and the origin such that the margin, i.e., the distance from the origin to the hyperplane, is maximized [24, 12]. The optimization problem is formulated as

$$\begin{aligned} & \max_{\mathbf{w}, \rho} \left( \frac{|\rho|}{\|\mathbf{w}\|^2} \right) \\ \text{s.t. : } & \mathbf{w}^\top \phi(x_i) - \rho \geq 0, i = 1, \dots, N \\ & \mathbf{w}^\top \mathbf{0} - \rho = -\rho < 0 \end{aligned}$$

where  $\phi$  is a transformation from the input space to the feature space and  $\mathbf{w}^\top \phi(x) - \rho = 0$  is equation of the hyperplane.

It occurs that the margin is invariant if we scale  $(\mathbf{w}, \rho)$  by a factor  $k$ . Hence without loss of generality, we can assume that  $\rho = 1$  and we achieve the following optimization problem

$$\begin{aligned} \min_{\mathbf{w}} \left( \frac{1}{2} \|\mathbf{w}\|^2 \right) \\ \text{s.t. : } \mathbf{w}^\top \phi(x_i) - 1 \geq 0, i = 1, \dots, N \end{aligned}$$

Using the slack variables, we can extend the above optimization problem to form the soft model of large margin one-class support vector machine (LM-OCSVM)

$$\begin{aligned} \min_{\mathbf{w}} \left( \frac{1}{2} \|\mathbf{w}\|^2 + \frac{C}{N} \sum_{i=1}^N \xi_i \right) \\ \text{s.t. : } \mathbf{w}^\top \phi(x_i) - 1 \geq -\xi_i, i = 1, \dots, N \\ \xi_i \geq 0, i = 1, \dots, N \end{aligned}$$

where  $C > 0$  is the trade-off parameter and  $\boldsymbol{\xi} = [\xi_1, \dots, \xi_N]$  is the vector of slack variables.

We can rewrite the above optimization problem in the primal form as follows

$$\min_{\mathbf{w}} \left( J(\mathbf{w}) \triangleq \frac{1}{2} \|\mathbf{w}\|^2 + \frac{C}{N} \sum_{i=1}^N \max \{0, 1 - \mathbf{w}^\top \phi(x_i)\} \right) \quad (1)$$

### 3. Budgeted stochastic gradient descent large margin one-class support vector machine

#### 3.1. Stochastic gradient descent solution

We can apply the stochastic gradient descent (SGD) framework to solve the optimization problem in Eq. (1) in its primal form. At the iteration  $t$ , we do the following steps:

- Uniformly sample  $n_t$  from  $[N] \triangleq \{1, 2, \dots, N\}$
- Construct the instantaneous objective function

$$\mathcal{J}_t(\mathbf{w}) = \frac{1}{2} \|\mathbf{w}\|^2 + C \max \{0, 1 - \mathbf{w}^\top \phi(x_{n_t})\}$$

- Set  $g_t = \mathcal{J}'_t(\mathbf{w}_t) = \mathbf{w}_t - C \mathbb{I}_{\mathbf{w}_t^\top \phi(x_{n_t}) < 1} \phi(x_{n_t})$  where  $\mathbb{I}_A$  is the indicator function, and is 1 if  $A$  is true and is 0 if otherwise
- Update  $\mathbf{w}_{t+1} = \mathbf{w}_t - \eta_t g_t = \frac{t-1}{t} \mathbf{w}_t + C \eta_t \mathbb{I}_{\mathbf{w}_t^\top \phi(x_{n_t}) < 1} \phi(x_{n_t})$  where  $\eta_t = \frac{1}{t}$  is the learning rate

---

**Algorithm 1** The pseudocode of stochastic gradient descent large margin one-class support vector machine.

---

**Input:**  $\mathcal{D}, K(\cdot, \cdot), C$

```

1:  $\mathbf{w}_1 = \mathbf{0}$ 
2: for  $t = 1$  to  $T$  do
3:   Sample  $n_t \sim \text{Uniform}([N])$ 
4:    $\mathbf{w}_{t+1} = \frac{t-1}{t} \mathbf{w}_t + C \eta_t \mathbb{I}_{\mathbf{w}^\top \phi(x_{n_t}) < 1} \phi(x_{n_t})$ 
5: end for

```

**Output:**  $\mathbf{w}_{T+1}$

---

The key steps of applying SGD to solve the optimization of LM-OCSVM in its primal form (cf. Eq. (1)) is summarized in Algorithm 1. At the iteration  $t$ , we uniformly sample a data instance from the training set and then update the model using this data instance. This kind of update enables the proposed algorithm to be performed in online mode and encourages an economic memory usage.

### 3.2. Budgeted stochastic gradient descent

The aforementioned update rule is vulnerable to the curse of kernelization, that is, the model size almost linearly grows up with the data size accumulated over time. This makes the computation is gradually slower across iterations and may cause potential memory overflow. To address this issue, we use the budget approach wherein a budget  $B$  is established and when the current model size exceeds this budget, a budget maintenance procedure is invoked to maintain the model size.

Algorithm 2 is proposed for BSGD-based Large Margin One-class Support Vector Machine (BSGD-LMOC). It is noteworthy that in Algorithm 2, we store  $\mathbf{w}_t$  as  $\sum_i \alpha_i \phi(x_i)$ . Whenever the current model size  $b$  exceeds the budget  $B$ , we invoke the procedure  $BM(\mathbf{w}_{t+1}, I_{t+1})$  to perform the budget maintenance so as to maintain the current model size  $b$  to the budget  $B$ . Here we note that  $I_{t+1}$  specifies the set of support indices during the iteration  $t$  (cf. Algorithm 2).

### 3.3. Budget maintenance strategies

In what follows, we present two budget maintenance strategies used in our article (i.e., removal and projection). The first strategy (i.e., removal) simply removes the most redundant vector. The second one projects the most redundant vector onto the linear span of the remaining vectors in the support set in the feature space before removing it. We assume that

$$\mathbf{w}_{t+1} = \sum_{i \in I_{t+1}} \alpha_i \phi(x_i)$$

The most redundant vector is determined as that with smallest coefficient as

$$p_t = \underset{i \in I_{t+1}}{\operatorname{argmin}} |\alpha_i| K(x_i, x_i)$$

---

**Algorithm 2** Algorithm for BSGD-LMOC

---

**Input:**  $C, B, K(\cdot, \cdot)$ 

```
1:  $\mathbf{w}_1 = \mathbf{0}$ 
2:  $b = 0$ 
3:  $I_1 = \emptyset$ 
4: for  $t = 1$  to  $T$  do
5:   Sample  $n_t$  from  $[N]$ 
6:   Update  $\mathbf{w}_{t+1} = \frac{t-1}{t}\mathbf{w}_t + \alpha_t\phi(x_{n_t})$  //  $\alpha_t = C\eta_t\mathbb{I}_{y_{n_t}\mathbf{w}_t^\top\phi(x_{n_t}) < \theta_{n_t}} y_{n_t}$ 
7:   if  $n_t \notin I_t$  and  $\alpha_t \neq 0$  then
8:      $b = b + 1$ 
9:      $I_{t+1} = I_t \cup \{n_t\}$ 
10:    if  $b > B$  then
11:       $\text{BM}(\mathbf{w}_{t+1}, I_{t+1})$  //Budget Maintenance
12:       $b = B$ 
13:    end if
14:  end if
15: end for
```

**Output:**  $\mathbf{w}_{T+1}$ 

---

### 3.3.1. Removal

The most redundant vector  $\phi(x_{p_t})$  is simply removed. It follows that

$$\mathbf{w}_{t+1} = \mathbf{w}_t - \alpha_{p_t}\phi(x_{p_t})$$

### 3.3.2. Projection

The full projection version used in [37] requires to invert a  $B$  by  $B$  matrix which costs  $O(B^3)$ . To reduce the incurred computation, we propose to project the most redundant vector  $\phi(x_{p_t})$  onto the set of  $k$  vectors in the feature space. This set of  $k$  vectors can be determined by either  $k$  nearest neighbor of  $x_{p_t}$  (i.e.,  $kNN(x_{p_t})$ ) in the input space or  $k$  random vectors (i.e.,  $kRD(x_{p_t})$ ) in the support set. The model  $\mathbf{w}_{t+1}$  is incremented by the projection of  $\phi(x_{p_t})$  onto the linear span of this set in the feature space. Finally, the most redundant vector is removed. In particular, we proceed as follows

$$\begin{aligned} kInd &= kNN(x_{p_t}, I_{t+1}) \text{ or } kRD(x_{p_t}, I_{t+1}) \\ P_t &= P(\phi(x_{p_t}), \text{span}(\phi(x_i) : i \in kInd)) \\ \mathbf{w}_{t+1} &= \mathbf{w}_t + \alpha_{p_t}P_t - \alpha_{p_t}\phi(x_{p_t}) \end{aligned}$$

It is noteworthy that the computational cost to find the projection  $P_t$  is  $O(k^3)$  where  $k$  is usually a small number (e.g.,  $k = 5$ ) comparing with the cost  $O(B^3)$  as in [37]. Since the projection has the form of  $P_t = \sum_{i \in kInd} d_i \phi(x_i)$ , the model size is recovered to  $B$  after performing the budget maintenance strategy.

### 3.4. Convergence analysis

In this section, we present the convergence analysis regarding the convergence rate of  $\mathbf{w}_t$  to the optimal solution  $\mathbf{w}^*$ . Without loss of generality, we assume that data are bounded in the feature space, i.e.,  $\|\phi(x)\| \leq R, \forall x \in \mathcal{X}$ . We now introduce the theoretical results below and shall leave all proofs to the appendix section. For comprehensibility, we make analysis for the removal case. Let us define  $Z_t$  to be the Bernoulli random variable which specifies if the budget maintenance is performed at round  $t$ . The update rule is as follows

$$\mathbf{w}_{t+1} = \mathbf{w}_t - \eta_t g_t - Z_t \alpha_{p_t} \phi(x_{p_t})$$

Lemmas 1, 2, 3, 4, and 6 establish the upper bound for the necessary quantities that need for the analysis. The main theorem 7 shows the upper bound on the regret.

**Lemma 1.** *Let us denote  $s_t = \sum_{i \in I_t} |\alpha_i|$ . We then have for all  $t$ ,*

$$s_t \leq CR$$

**Lemma 2.** *The following statement holds for all  $t$ ,*

$$\|\mathbf{w}_t\| \leq CR^2$$

**Lemma 3.** *The following statement holds for all  $t$ ,*

$$\|g_t\| \leq G = CR + CR^2$$

**Lemma 4.** *Given a positive number  $m$ , assume that before removing  $(x_{p_t}, y_{p_t})$  is updated at most  $m$  times. We then have the following statement for all  $t$ ,*

$$|\alpha_{p_t}| \leq \frac{mCR}{t}$$

**Lemma 5.** *Let us denote  $\rho_i = \frac{\alpha_i}{\eta_t} = t\alpha_i, \forall i \in I_t$  and  $h_t = Z_t \rho_{p_t} \phi(x_{p_t})$ . We then have*

$$\|h_t\| \leq H = mCR^2$$

**Lemma 6.** *We have the following inequality for all  $t$ ,*

$$\mathbb{E} \left[ \|\mathbf{w}_t - \mathbf{w}^*\|^2 \right] \leq W^2 = \left( H + \sqrt{H^2 + (G + H)^2} \right)^2$$

**Theorem 7.** *Considering the running of Algorithm 2, we have the following inequality*

$$\begin{aligned} \mathbb{E}[\mathcal{J}(\bar{\mathbf{w}}_T)] - \mathcal{J}(\mathbf{w}^*) &\leq \frac{1}{T} \sum_{t=1}^T \mathbb{E}[\mathcal{J}(\mathbf{w}_t)] - \mathcal{J}(\mathbf{w}^*) \\ &\leq \frac{(G + H)^2 (\log T + 1)}{2T} + \frac{WR}{T} \sum_{t=1}^T \mathbb{P}(Z_t = 1) \mathbb{E}[\rho_{p_t}^2]^{1/2} \end{aligned}$$

Theorem 7 reveals that there exists an error gap between the outputting solution and the optimal solution. This gap crucially depends on the budget maintenance rate  $\mathbb{P}(Z_t = 1)$  and the gradient error  $\rho_{p_t} = \frac{\alpha_{p_t}}{\eta_t}$ . It also discloses that we need to remove the vector with smallest absolute coefficient (i.e.,  $|\alpha_{p_t}|$ ) to rapidly reduce the error gap.

It is noteworthy that our analysis also covers the standard analysis. In particular, when the budget maintenance never happens (i.e.,  $\mathbb{P}(Z_t = 1) = 0$ ), we gain the typical convergence rate  $O\left(\frac{\log T}{T}\right)$ .

#### 4. Clustering assignment

After solving the optimization problem, we yield the decision function

$$f(x) = \sum_{i=1}^N \alpha_i K(x_i, x) - 1$$

To find the equilibrium points, we need to solve the equation  $\nabla f(x) = 0$ . To this end, we use the fixed point technique and assume that Gaussian kernel is used, i.e.,  $K(x, x') = e^{-\gamma\|x-x'\|^2}$ . We then have

$$\frac{1}{2}\nabla f(x) = \sum_{i=1}^N \alpha_i (x_i - x) e^{-\gamma\|x-x_i\|^2} = 0 \rightarrow x = \frac{\sum_{i=1}^N \alpha_i e^{-\gamma\|x-x_i\|^2} x_i}{\sum_{i=1}^N \alpha_i e^{-\gamma\|x-x_i\|^2}} = P(x)$$

To find an equilibrium point, we start with the initial point  $x^{(0)} \in \mathbb{R}^d$  and iterate  $x^{(j+1)} = P(x^{(j)})$ . By fixed point theorem, the sequence  $x^{(j)}$ , which can be considered as a trajectory with start  $x^{(0)}$ , converges to the point  $x_*^{(0)}$  satisfying  $P(x_*^{(0)}) = x_*^{(0)}$  or  $\nabla f(x_*^{(0)}) = 0$ , i.e.,  $x_*^{(0)}$  is an equilibrium point.

Let us denote  $B_\epsilon = \{x_i : 1 \leq i \leq N \wedge |f(x_i)| \leq \epsilon\}$ , namely the extended boundary for a tolerance  $\epsilon > 0$ . It follows that the set  $B_\epsilon$  forms a strip enclosing the decision boundary  $f(x) = 0$ . Algorithm 3 is proposed to do clustering assignment. In Algorithm 3, the task of clustering assignment is reduced to itself for  $M$  equilibrium points. To fulfill cluster assignment for  $M$  equilibrium points, we run  $m = 20$  sample-point test as proposed in [1].

Our proposed clustering assignment procedure is different from the existing procedure proposed in [1]. The procedure proposed in [1] requires to run  $m = 20$  sample-point test for every edge connected  $x_i, x_j$  ( $i \neq j$ ) in the training set. Consequently, the computational cost incurred is  $O(N(N-1)ms)$  where  $s$  is the sparsity level of the decision function (i.e., the number of vectors in the model). Our proposed procedure needs to perform  $m = 20$  sample-point test for a reduced set of  $M$  data samples (i.e., the set of the equilibrium points  $\{e_1, e_2, \dots, e_M\}$ ) where  $M$  is possibly very small comparing with  $N$ . The reason is that many data points in the training set could converge to a common equilibrium point which significantly reduces the size from  $N$  to  $M$ . The computational cost incurred is therefore  $O(M(M-1)ms)$ .



---

**Algorithm 3** Clustering assignment procedure.

---

**Input:**  $f(x) = \sum_{i=1}^N \alpha_i K(x_i, x) - 1$ ,  $B_\epsilon$ 

```
1:  $E = \emptyset$ 
2: for  $x^{(0)}$  in  $B_\epsilon$  do
3:   Find the equilibrium point  $x_*^{(0)}$ 
4:   if  $x_*^{(0)} \notin E$  then
5:      $E = E \cup \{x_*^{(0)}\}$ 
6:   end if
7: end for
8: Do  $m$  sample point test for  $E$  to find cluster indices for  $e_1, e_2, \dots, e_M$ 
   // Assume that  $E = \{e_1, e_2, \dots, e_M\}$ 
9: Each point  $x^{(0)} \in B_\epsilon$  is assigned to the cluster of its corresponding equilibrium point  $x_*^{(0)} \in E$ 
10: Each point  $x \in \mathcal{D} \setminus B_\epsilon$  is assigned to the cluster of its nearest neighbor in  $B_\epsilon$  using the Euclidean distance
```

---

**Output:** clustering solution for  $\mathcal{D} = \{x_1, \dots, x_N\}$ 

---

## 5. Experiments

### 5.1. Visual experiment

To visually show the high clustering quality produced by our proposed method using budgeted SGD in conjunction with the removal strategy, we establish experiment on three synthesized datasets and visually make comparison of the proposed method with C-Means and Fuzzy C-Means. In the first experiment, data samples form the nested structure with two outside rings and one Gaussian distribution at center. As shown in Fig. 1, our method can perfectly detect three clusters without any prior information whilst both C-Means and Fuzzy C-Means with the number of clusters being set to 3 beforehand fail to discover the nested clusters. The second experiment is carried out with a two-moon dataset. As observed from Fig. 2, our method without any prior knowledge can perfectly discover two clusters in moons. However, C-Means and Fuzzy C-Means cannot detect the clusters correctly. In the last visual experiment, we generate data from the mixture of 3 or 4 Gaussian distributions. As shown in Fig. 3, our method can perfectly detect 3 (left) and 4 (right) clusters corresponding to the individual Gaussian distributions. These visual experiments demonstrate that the proposed method is able to not only generate the cluster boundaries in arbitrary shapes but also automatically detect the appropriate number of clusters well presented the data.

### 5.2. Experiment on real datasets

To explicitly prove the performance of the proposed algorithm, we conduct experiments on the real datasets. Cluster analysis is naturally an unsupervised learning task and therefore, there does not exist a perfect measure to compare given two clustering algorithms. We make use of five typical clustering validity

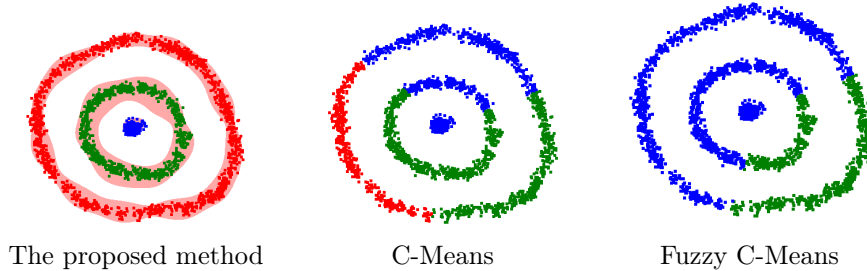


Figure 1: Visual comparison of the proposed method (the orange region is the domain of novelty) with C-Means and Fuzzy C-Means on two ring dataset.

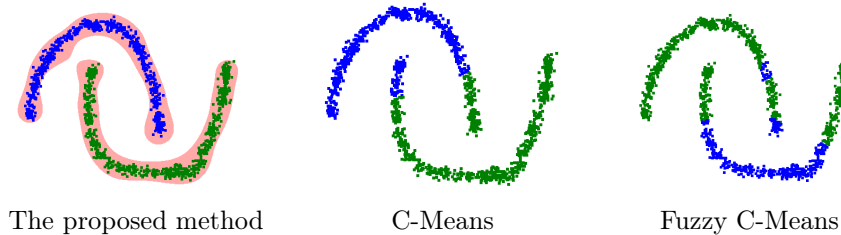


Figure 2: Visual comparison of the proposed method (the orange region is the domain of novelty) with C-Means and Fuzzy C-Means on two moon dataset.

indices (CVI) including compactness, purity, rand index, Davies-Bouldin index (DB index), and normalized mutual information (NMI) for comparison. A good clustering algorithm should achieve a solution which has a high purity, rand index, DB index, and NMI and a low compactness.

#### *Clustering validity index*

Compactness measures the average pairwise distances of points in the same cluster [6] and is given as follows

$$Compactness \triangleq \frac{1}{N} \sum_{k=1}^m N_k \frac{\sum_{x, x' \in C_k} d(x, x')}{N_k (N_k - 1) / 2}$$

where the cluster solution consists of  $m$  clusters  $C_1, C_2, \dots, C_m$  whose cardinalities are  $N_1, N_2, \dots, N_m$ , respectively.

The clustering with a small compactness is preferred. A small compactness gained means the average intra-distance of clusters is small and homogeneity is thereby good, i.e., two objects in the same cluster has high similarity to each other.

The second CVI in use is purity which measures the purity of clustering solution with respect to the nature classes of data [23]. It is certainly true that the metric purity is only appropriate for data with labels in nature. Let  $N_{ij}$  be the number of objects in cluster  $i$  that belong to the class  $j$ . Again, let

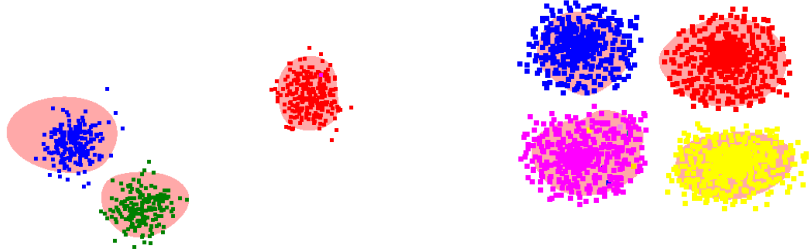


Figure 3: The proposed method (the orange region is the domain of novelty) can recognize the clusters scattered from mixture of either 3 (left) or 4 (right) Gaussian distributions.

$N_i \triangleq \sum_{j=1}^m N_{ij}$  be total number of objects in cluster  $i$ . Let us define  $p_{ij} \triangleq \frac{N_{ij}}{N_j}$ , i.e., the empirical distribution over class labels for cluster  $i$ . We define a purity of a cluster as  $p_i \triangleq \max_j p_{ij}$  and overall purity of a clustering solution as

$$Purity \triangleq \sum_i \frac{N_i}{N} \times p_i$$

The purity ranges between 0 (bad) and 1 (good). This CVI embodies the classification ability of clustering algorithm. A clustering algorithm which achieves a high purity can be appropriately used for classification purpose.

The third CVI used as a measure is rand index [23]. To calculate this CVI for a clustering solution, we need to construct a  $2 \times 2$  contingency table containing the following numbers: 1) TP (true positive) is the number of pairs that are in the same cluster and belong to the same class; 2) TN (true negative) is the number of pairs that are in two different clusters and belong to different classes; 3) FP (false positive) is the number of pairs that are in the same cluster but belong to different classes; and 4) FN (false negative) is the number of pairs that are in two different clusters but belong to the same class. Rand index is defined as follows

$$Rand \triangleq \frac{TP + TN}{TP + FP + TN + FN}$$

This can be interpreted as the fraction of clustering decisions that are correct. Obviously, rand index ranges between 0 and 1.

Davies-Bouldin validity index is a function of the ratio of the sum of intra-distances to inter-distances [6] and is formulated as follows

$$DBI \triangleq \frac{1}{m} \sum_{i=1}^m \max_{j \neq i} \left\{ \frac{\Delta(C_i) + \Delta(C_j)}{d(C_i, C_j)} \right\}$$

A good clustering algorithm should produce the solution which has as small DBI as possible.

The last considered CVI is normalized mutual information (NMI) [23]. This measure allows us to trade off the quality of the clustering against the number of clusters.

$$NMI \triangleq \frac{I(\Omega, C)}{[H(C) + H(\Omega)]/2}$$

where  $C = \{c_1, \dots, c_J\}$  is the set of classes and  $\Omega = \{\omega_1, \dots, \omega_K\}$  is the set of clusters.

$I(\Omega, C)$  is the mutual information and is defined as

$$I(\Omega, C) \triangleq \sum_k \sum_j P(c_j \cap \omega_k) \log \frac{P(c_j \cap \omega_k)}{P(c_j)P(\omega_k)}$$

and  $H(\cdot)$  is the entropy and is defined as

$$H(\Omega) \triangleq - \sum_k P(\omega_k) \log P(\omega_k)$$

It is certainly that the NMI ranges between 0 and 1, and a good clustering algorithm should produce as high NMI measure as possible.

We perform experiments on 15 well-known datasets for clustering task. The statistics of the experimental datasets is given in Table 1. These datasets are fully labeled and consequently, the CVIs like purity, rand index, and NMI can be completely estimated. We make comparison of our proposed method with the following baselines.

Datasets	Size	Dimension	#Classes
Aggregation	788	2	7
Breast Cancer	699	9	2
Compound	399	2	6
D31	3,100	2	31
Flame	240	2	2
Glass	214	9	7
Iris	150	4	3
Jain	373	2	2
Pathbased	300	2	3
R15	600	2	15
Spiral	312	2	3
Abalone	4,177	8	28
Car	1,728	6	4
Musk	6,598	198	2
Shuttle	43,500	9	5

Table 1: The statistics of the experimental datasets.

#### Baselines

- *Support vector clustering (SVC)* [1]: using LIBSVM [4] to find domain of novelty and fully connected graph for clustering assignment.

- *Fast support vector clustering (FSVC)* [9]: an equilibrium-based approach for clustering assignment.
- *SGD Large Margin One-class Support Vector Machine (SGD-LMOC)* [28]: the SGD-based solution of Large Margin One-class Support Vector Machine which is vulnerable to the curse of kernelization.

Our proposed method has three variants which correspond to three budget maintenance strategies. We name these three variants as BSGD-R (BSGD + removal strategy), BSGD-PNN (BSGD + projection strategy with  $k$ -nearest neighbors), and BSGD-PRN (BSGD + projection strategy with  $k$ -random neighbors). It is noteworthy that we use BSGD-R, BSGD-PNN, or BSGD-PRN (cf. Algorithm 2 and Section 3.3) to train the model in the first phase and then use Algorithm 3 to perform clustering assignment in the second phase. All competitive methods are run on a Windows computer with dual-core CPU 2.6GHz and 4GB RAM.

#### Hyperparameter Setting

The RBF kernel, given by  $K(x, x') = e^{-\gamma \|x - x'\|^2}$ , is employed. The width of kernel  $\gamma$  is searched on the grid  $\{2^{-5}, 2^{-3}, \dots, 2^3, 2^5\}$ . The trade-off parameter  $C$  is searched on the same grid. In addition, the parameters  $p$  and  $\varepsilon$  in FSVC are searched in the common grid  $\{0.1, 0.2, \dots, 0.9, 1\}$  which is the same as in [9]. Determining the number of iterations in Algorithm 2 is really challenging. To resolve it, we use the stopping criterion  $\|\mathbf{w}_{t+1} - \mathbf{w}_t\| \leq \theta = 0.01$  (i.e., the next hyperplane does only a slight change). For the projection strategy in BSGD-PNN and BSGD-PRN, we set  $k = 5$  to efficiently relax the matrix inversion.

#### Experimental Result

Dataset	Purity					
	SVC	SGD	FSVC	BSGD-R	BSGD-PNN	BSGD-PRN
Aggregation [50]	<b>1.00</b>	<b>1.00</b>	0.22	<b>1.00</b>	<b>1.00</b>	<b>1.00</b>
Breast Cancer [50]	0.98	<b>0.99</b>	<b>0.99</b>	0.95	<b>0.99</b>	0.97
Compound [50]	0.66	0.62	0.13	<b>0.99</b>	0.98	0.97
Flame [50]	0.86	0.87	0.03	<b>1.00</b>	<b>1.00</b>	<b>1.00</b>
Glass [50]	0.50	0.71	0.65	0.88	0.87	<b>0.93</b>
Iris [50]	<b>1.00</b>	<b>1.00</b>	0.68	<b>1.00</b>	<b>1.00</b>	0.99
Jain [50]	0.37	0.46	0.69	<b>1.00</b>	<b>1.00</b>	<b>1.00</b>
Pathbased [50]	0.60	0.50	<b>1.00</b>	<b>1.00</b>	<b>1.00</b>	<b>1.00</b>
R15 [50]	0.88	0.90	0.37	<b>1.00</b>	0.99	<b>1.00</b>
Spiral [50]	0.09	0.33	0.53	<b>1.00</b>	<b>1.00</b>	<b>1.00</b>
D31 [50]	0.94	<b>0.99</b>	0.42	0.96	0.97	0.91
Abalone [50]	0.22	0.44	0.03	0.33	<b>0.57</b>	0.36
Car [50]	0.94	<b>0.95</b>	0.70	0.91	0.83	0.86
Musk [50]	0.87	0.68	<b>0.88</b>	0.42	0.64	0.60
Shuttle [100]	0.06	0.05	0.06	0.34	<b>0.90</b>	0.42

Table 2: The purity of the clustering methods on the experimental datasets. Larger is better. The number (i.e., [x]) nearby the dataset name specifies the budget size used in the proposed method.

Dataset	Rand Index					
	SVC	SGD	FSVC	BSGD-R	BSGD-PNN	BSGD-PRN
Aggregation [50]	<b>1.00</b>	<b>1.00</b>	0.22	0.94	0.93	0.95
Breast Cancer [50]	0.82	<b>0.85</b>	0.81	0.73	0.78	0.72
Compound [50]	0.92	0.88	0.25	0.90	<b>0.95</b>	0.91
Flame [50]	0.75	0.76	0.03	0.87	0.74	<b>0.91</b>
Glass [50]	0.77	<b>0.91</b>	0.54	0.78	0.83	0.81
Iris [50]	<b>0.97</b>	0.96	0.69	0.83	0.84	0.81
Jain [50]	0.70	0.71	0.77	<b>1.00</b>	0.98	0.89
Pathbased [50]	0.81	<b>0.94</b>	1.00	0.71	0.77	0.76
R15 [50]	0.74	0.71	0.37	0.95	0.95	<b>0.96</b>
Spiral [50]	0.15	<b>0.94</b>	0.75	0.91	0.75	0.75
D31 [50]	0.88	0.81	0.54	<b>0.98</b>	<b>0.98</b>	0.96
Abalone [50]	0.43	0.86	0.12	0.88	<b>0.89</b>	0.88
Car [50]	0.46	0.46	0.54	0.55	0.56	<b>0.59</b>
Musk [50]	0.26	0.28	0.26	0.74	<b>0.76</b>	0.75
Shuttle [100]	<b>0.84</b>	0.83	0.75	0.50	0.62	0.63

Table 3: The rand index of the clustering methods on the experimental datasets. Larger is better. The number (i.e., [x]) nearby the dataset name specifies the budget size used in the proposed method.

Dataset	NMI					
	SVC	SGD	FSVC	BSGD-R	BSGD-PNN	BSGD-PRN
Aggregation [50]	0.69	0.75	0.60	<b>0.89</b>	<b>0.89</b>	<b>0.89</b>
Breast Cancer [50]	0.22	<b>0.55</b>	0.45	0.42	0.43	0.41
Compound [50]	0.51	0.81	0.45	<b>0.82</b>	<b>0.82</b>	0.77
Flame [50]	0.55	0.51	0.05	0.57	0.54	<b>0.66</b>
Glass [50]	<b>0.60</b>	0.44	0.53	0.55	0.54	0.56
Iris [50]	0.63	0.75	0.71	<b>0.76</b>	<b>0.76</b>	<b>0.76</b>
Jain [50]	0.53	0.31	<b>1.00</b>	0.98	0.92	0.68
Pathbased [50]	0.48	0.43	0.12	0.49	<b>0.58</b>	0.52
R15 [50]	0.67	0.77	0.77	0.80	<b>0.83</b>	0.80
Spiral [50]	0.52	0.34	0.16	<b>0.85</b>	0.58	0.59
D31 [50]	0.45	0.50	0.38	0.80	0.81	<b>0.89</b>
Abalone [50]	0.22	<b>0.34</b>	0.07	0.27	0.31	0.28
Car [50]	0.32	0.32	0.24	<b>0.33</b>	0.33	0.29
Musk [50]	0.21	0.16	<b>0.23</b>	0.08	0.14	0.11
Shuttle [100]	0.26	0.41	0.50	0.38	0.47	<b>0.52</b>

Table 4: The NMI of the clustering methods on the experimental datasets. Larger is better. The number (i.e., [x]) nearby the dataset name specifies the budget size used in the proposed method.

Dataset	Compactness					
	SVC	SGD	FSVC	BSGD-R	BSGD-PNN	BSGD-PRN
Aggregation [50]	0.29	0.29	2.84	<b>0.01</b>	<b>0.01</b>	0.02
Breast Cancer [50]	1.26	0.68	<b>0.71</b>	2.17	1.04	2.18
Compound [50]	0.5	0.21	2.43	0.02	<b>0.01</b>	0.03
Flame [50]	0.58	0.44	2.28	<b>0.03</b>	<b>0.03</b>	<b>0.03</b>
Glass [50]	0.72	0.68	1.85	0.75	0.69	<b>0.34</b>
Iris [50]	0.98	0.25	0.99	0.02	<b>0.01</b>	0.05
Jain [50]	0.96	0.36	1.16	<b>0.01</b>	<b>0.01</b>	<b>0.01</b>
Pathbased [50]	0.18	0.3	1.04	<b>0.01</b>	<b>0.01</b>	<b>0.01</b>
R15 [50]	0.61	0.13	1.84	<b>0.01</b>	<b>0.01</b>	<b>0.01</b>
Spiral [50]	2.00	0.17	0.18	<b>0.01</b>	<b>0.01</b>	0.02
D31 [50]	1.41	0.26	1.78	<b>0.01</b>	<b>0.01</b>	0.25
Abalone [50]	3.88	0.40	4.97	0.23	<b>0.15</b>	0.21
Car [50]	0.75	<b>0.74</b>	14.68	1.32	3.06	5.25
Musk [50]	<b>9.89</b>	30.05	20.00	100.16	31.17	40.42
Shuttle [100]	0.50	0.46	<b>0.26</b>	0.28	0.50	0.50

Table 5: The compactness of the clustering methods on the experimental datasets. Smaller is better. The number (i.e., [x]) nearby the dataset name specifies the budget size used in the proposed method.

Dataset	DB Index					
	SVC	SGD	FSVC	BSGD-R	BSGD-PNN	BSGD-PRN
Aggregation [50]	0.68	0.67	0.63	4.45	<b>4.53</b>	3.99
Breast Cancer [50]	1.58	1.38	0.53	4.80	4.64	<b>5.71</b>
Compound [50]	2.45	0.86	0.67	3.84	<b>5.15</b>	3.01
Flame [50]	1.30	0.65	3.56	3.42	<b>4.01</b>	3.29
Glass [50]	0.53	0.56	0.93	3.98	<b>4.64</b>	4.14
Iris [50]	1.95	1.17	0.77	3.42	<b>3.96</b>	3.44
Jain [50]	1.23	1.08	0.71	4.38	4.19	<b>4.22</b>
Pathbased [50]	0.36	0.73	1.07	4.02	<b>4.42</b>	3.71
R15 [50]	2.96	1.42	1.37	4.00	<b>4.33</b>	3.91
Spiral [50]	1.41	0.98	0.36	5.38	4.69	<b>5.66</b>
D31 [50]	2.33	1.35	1.21	4.40	<b>5.36</b>	3.35
Abalone [50]	3.78	3.91	1.29	6.28	<b>6.32</b>	6.27
Car [50]	1.76	1.76	1.57	<b>3.02</b>	3.00	2.97
Musk [50]	2.27	2.83	0.01	2.69	<b>3.87</b>	3.64
Shuttle [100]	1.86	1.84	1.32	<b>4.04</b>	3.66	3.71

Table 6: The DB index of the clustering methods on the experimental datasets. Larger is better. The number (i.e., [x]) nearby the dataset name specifies the budget size used in the proposed method.

Dataset	Training Time					
	SVC	SGD	FSVC	BSGD-R	BSGD-PNN	BSGD-PRN
Aggregation [50]	0.05	0.03	0.05	<b>0.01</b>	0.02	0.03
Breast Cancer [50]	0.18	<b>0.02</b>	0.05	<b>0.02</b>	0.03	0.04
Compound [50]	0.03	0.02	0.10	<b>0.01</b>	<b>0.01</b>	<b>0.01</b>
Flame [50]	0.02	0.02	15.16	<b>0.01</b>	<b>0.01</b>	<b>0.01</b>
Glass [50]	0.03	0.03	0.02	<b>0.01</b>	<b>0.01</b>	<b>0.01</b>
Iris [50]	0.02	0.02	0.04	<b>0.01</b>	<b>0.01</b>	<b>0.01</b>
Jain [50]	0.02	0.02	0.03	<b>0.01</b>	<b>0.01</b>	<b>0.01</b>
Pathbased [50]	0.02	0.02	0.05	<b>0.01</b>	<b>0.01</b>	<b>0.01</b>
R15 [50]	0.02	0.02	0.02	<b>0.01</b>	<b>0.01</b>	0.02
Spiral [50]	0.02	0.03	0.02	<b>0.01</b>	<b>0.01</b>	<b>0.01</b>
D31 [50]	0.17	<b>0.09</b>	<b>0.09</b>	0.13	0.16	0.11
Abalone [50]	2.26	0.81	10.94	0.36	0.27	<b>0.22</b>
Car [50]	5.62	0.64	8.15	<b>0.05</b>	0.06	0.07
Musk [50]	55.93	5.79	58.49	<b>1.36</b>	1.89	1.43
Shuttle [100]	10.03	<b>0.46</b>	68.43	1.51	2.15	1.82

Table 7: The training time (in second) of the clustering methods on the experimental datasets. Shorter is better. The number (i.e., [x]) nearby the dataset name specifies the budget size used in the proposed method.

Dataset	Clustering Time					
	SVC	SGD	FSVC	BSGD-R	BSGD-PNN	BSGD-PRN
Aggregation [50]	31.42	2.83	7.51	<b>0.37</b>	0.61	1.43
Breast Cancer [50]	19.80	2.14	22.86	<b>0.29</b>	0.62	1.48
Compound [50]	6.82	1.17	7.24	<b>0.11</b>	0.15	0.51
Flame [50]	1.81	0.67	4.31	<b>0.05</b>	0.08	0.24
Glass [50]	2.30	0.53	10.67	<b>0.06</b>	0.09	0.41
Iris [50]	1.03	0.34	4.33	<b>0.03</b>	<b>0.03</b>	0.15
Jain [50]	5.80	0.81	4.59	<b>0.10</b>	0.16	0.45
Pathbased [50]	4.02	0.54	4.22	<b>0.06</b>	0.09	0.33
R15 [50]	4.14	3.68	10.43	<b>0.22</b>	0.35	0.94
Spiral [50]	1.60	0.99	7.78	<b>0.07</b>	0.10	0.35
D31 [50]	467.72	6.56	33.08	<b>4.58</b>	8.39	13.33
Abalone [50]	653.65	26.58	242.97	3.79	<b>1.84</b>	5.57
Car [50]	67.66	<b>7.05</b>	84.47	16.24	8.42	23.57
Musk [50]	602.09	432.58	510.25	<b>173.36</b>	194.69	183.78
Shuttle [100]	1,972.61	<b>925</b>	1,125.46	1,766.66	1,739.62	1,759.06

Table 8: The clustering time (in second) of the clustering methods on the experimental datasets. Shorter is better. The number (i.e., [x]) nearby the dataset name specifies the budget size used in the proposed method.

We use 5 cluster validation indices including purity, rand index, NMI, DB index, and compactness to compare the proposed method with the baselines. Each experiment is carried out 5 times and the averages of the cluster validation indices are reported. For readability, we emphasize in boldface the method that yields the best CVI for each dataset. Regarding purity (cf. Table 2), our proposed method outperforms other baselines. Its three variants obtain the best purity on 12 out of 15 experimental datasets. This fact also indicates a good classification ability of the proposed method. Hence, the proposed method including its three variants can be certainly used for classification purpose. As



regards rand index (cf. Table 3), the proposed method gains comparable results in comparison to the baselines. In reference to NMI (cf. Table 4), the proposed method is again comparable with the baselines. In particular, its three variants win over 10 out of 15 experimental datasets. The proposed method including its three variants also attains very convincing compactness indices comparing with the baselines (cf. Table 5). In particular, its three variants surpass others on 11 experimental datasets. The last reported CVI is DB index. The proposed method dominates others on this CVI (cf. Table 6). In particular, it exceeds others on all experimental datasets. Regarding the amount of time taken for finding the domain of novelty, the proposed method especially the variant BSGD-R is faster than the baselines on most datasets. The proposed method and SGD-LMOC [28] are SGD-based method but because of its sparser model, the proposed method is faster than SGD-LMOC whilst preserving the learning performance of this method. In regards to the cluster time, the proposed method again outperforms the baselines. Comparing among three variants of the proposed method, BSGD-R (i.e., removal strategy) is faster than others. It is reasonable from the simplicity of this strategy. The BSGD-PNN variant (i.e., projection with  $k$ -nearest neighbors) is a little slower than the BSGD-PRN (i.e., projection with  $k$ -random neighbors). The reason lies in the fact that BSGD-PNN needs to sort out the support vectors in the model which raises more computational burden.

## 6. Conclusion

In this paper, we have proposed a scalable support-based clustering method, which conjoins the advantages of SGD-based method, kernel-based method, and budget approach. Furthermore, we have also proposed a new strategy for clustering assignment. We have validated our proposed method on 15 well-known datasets for clustering. The experimental results have shown that our proposed method has achieved the comparable clustering quality comparing with the baseline whilst being much faster.

## References

### References

- [1] A. Ben-Hur, D. Horn, H. T. Siegelmann, and V. Vapnik. Support vector clustering. *J. Mach. Learn. Res* 2, 2:125–137, 2001.
- [2] F. Camastra and A. Verri. A novel kernel method for clustering. *IEEE Trans. Pattern Anal. Mach. Intell.*, 27(5):801–804, 2005.
- [3] G. Cavallanti, N. Cesa-Bianchi, and C. Gentile. Tracking the best hyperplane with a simple budget perceptron. *Machine Learning*, 69(2-3):143–167, 2007.
- [4] C.-C. Chang and C.-J. Lin. libsvm: a library for support vector machines. *ACM Trans. Intell. Syst. Technol.*, 2(3):27:1–27:27, 2011.
- [5] K. Crammer, J. Kandola, and Y. Singer. Online classification on a budget. In *Advances in Neural Information Processing Systems 16*. MIT Press, 2004.
- [6] M. Halkidi, Y. Batistakis, and M. Vazirgiannis. Clustering validity checking methods: Part ii. *SIGMOD Rec.*, 31(3):19–27, September 2002.
- [7] E. Hazan and S. Kale. Beyond the regret minimization barrier: optimal algorithms for stochastic strongly-convex optimization. *J. Mach. Learn. Res.*, 15(1):2489–2512, 2014.
- [8] T. Joachims. Advances in kernel methods. In. chapter Making Large-Scale Support Vector Machine Learning Practical, pages 169–184. 1999.
- [9] K.-H. Jung, D. Lee, and J. Lee. Fast support-based clustering method for large-scale problems. *Pattern Recognit.*, 43(5):1975–1983, 2010.
- [10] T. Le, P. Duong, M. Dinh, T. D. Nguyen, V. Nguyen, and D. Phung. Budgeted semi-supervised support vector machine. In *The Conference on Uncertainty in Artificial Intelligence (UAI)*, 2016.
- [11] T. Le, V. Nguyen, D. T. Nguyen, and D. Phung. Nonparametric budgeted stochastic gradient descent. In *Proceedings of the 19th International Conference on Artificial Intelligence and Statistics*, pages 654–662, 2016.
- [12] T. Le, V. Nguyen, T. Pham, M. Dinh, and T. H. Le. *Fuzzy Semi-supervised Large Margin One-Class Support Vector Machine*, pages 65–78. Springer International Publishing, 2015.
- [13] T. Le, D. Tran, W. Ma, and D. Sharma. An optimal sphere and two large margins approach for novelty detection. In *The 2010 International Joint Conference on Neural Networks*.

- [14] T. Le, D. Tran, P. Nguyen, W. Ma, and D. Sharma. Proximity multi-sphere support vector clustering. *22(7-8):1309–1319*, 2013.
- [15] Trung Le, Tu Nguyen, Vu Nguyen, and Dinh Phung. Dual space gradient descent for online learning. In *Advances in Neural Information Processing Systems (NIPS)*, pages 4583–4591, 2016.
- [16] Trung Le, Tu Dinh Nguyen, Vu Nguyen, and Dinh Phung. Approximation vector machines for large-scale online learning. *Journal of Machine Learning Research (JMLR)*, 2017.
- [17] Trung Le, Dat Tran, Tuan Hoang, Wanli Ma, and Dharmendra Sharma. Generalised support vector machine for brain-computer interface. In *International Conference on Neural Information Processing (ICONIP)*, pages 692–700. Springer, 2011.
- [18] Trung Le, Dat Tran, and Wanli Ma. Fuzzy multi-sphere support vector data description. In *Pacific-Asia Conference on Knowledge Discovery and Data Mining (PAKDD)*, pages 570–581. Springer, 2013.
- [19] Trung Le, Dat Tran, Tien Tran, Khanh Nguyen, and Wanli Ma. Fuzzy entropy semi-supervised support vector data description. In *International Joint Conference on Neural Networks (IJCNN)*, pages 1–5. IEEE, 2013.
- [20] J. Lee and D. Lee. An improved cluster labeling method for support vector clustering. *IEEE Trans. Pattern Anal. Mach. Intell.*, 27(3):461–464, March 2005.
- [21] J. Lee and D. Lee. Dynamic characterization of cluster structures for robust and inductive support vector clustering. *IEEE Trans. Pattern Anal. Mach. Intell.*, 28(11):1869–1874, November 2006.
- [22] H. Li. A fast and stable cluster labeling method for support vector clustering. *J. Comput.*, 8(12):3251–3256, 2013.
- [23] K. P. Murphy. *Machine Learning: A Probabilistic Perspective*. The MIT Press, 2012.
- [24] V. Nguyen, T. Le, T. Pham, M. Dinh, and T. H. Le. Kernel-based semi-supervised learning for novelty detection. In *2014 International Joint Conference on Neural Networks (IJCNN)*, pages 4129–4136, July 2014.
- [25] Van Nguyen, Trung Le, Thien Pham, Mi Dinh, and Thai Hoangi Le. Kernel-based semi-supervised learning for novelty detection. In *International Joint Conference on Neural Networks (IJCNN)*, pages 4129–4136. IEEE, 2014.
- [26] J.H. Park, X. Ji, H. Zha, and R. Kasturi. Support vector clustering combined with spectral graph partitioning. pages 581–584, 2004.
- [27] T. Pham, H. Dang, T. Le, and T. H. Le. Fast support vector clustering. *Vietnam Journal of Computer Science*, pages 1–9, 2016.

- [28] T. Pham, T. Le, H. T. Le, and D. Tran. Fast support vector clustering. In *European Symposium on Artificial Neural Networks, Computational Intelligence and Machine Learning*, 2016.
- [29] J. C. Platt. Advances in kernel methods. chapter Fast Training of Support Vector Machines Using Sequential Minimal Optimization, pages 185–208. 1999.
- [30] H. Robbins and S. Monro. A stochastic approximation method. *Annals of Mathematical Statistics*, 22:400–407, 1951.
- [31] B. Schölkopf, J. C. Platt, J. C. Shawe-Taylor, A. J. Smola, and R. C. Williamson. Estimating the support of a high-dimensional distribution. *Neural Comput.*, 13(7):1443–1471, July 2001.
- [32] S. Shalev-Shwartz and S. M. Kakade. Mind the duality gap: Logarithmic regret algorithms for online optimization. In *NIPS*, pages 1457–1464, 2008.
- [33] S. Shalev-Shwartz and Y. Singer. Logarithmic regret algorithms for strongly convex repeated games. In *The Hebrew University*, 2007.
- [34] S. Shalev-Shwartz, Y. Singer, and N. Srebro. Pegasos: Primal estimated sub-gradient solver for svm. In *In ICML*, pages 807–814, 2007.
- [35] R. Shamir and R. Sharan. Algorithmic approaches to clustering gene expression data. In *Current Topics in Computational Biology*, pages 269–300. MIT Press, 2001.
- [36] D. M.J. Tax and R. P.W. Duin. Support vector data description. *Machine learning*, 54(1):45–66, 2004.
- [37] Z. Wang, K. Crammer, and S. Vucetic. Breaking the curse of kernelization: Budgeted stochastic gradient descent for large-scale svm training. *Journal of Machine Learning Research*, 13(1):3103–3131, 2012.
- [38] Z. Wang and S. Vucetic. Online passive-aggressive algorithms on a budget. In *AISTATS*, volume 9, pages 908–915, 2010.
- [39] J. Yang, V. Estivill-Castro, and S. K. Chalup. Support vector clustering through proximity graph modelling. In *Neural Information Processing, 2002. ICONIP'02*, volume 2, pages 898–903, 2002.

## Appendix A. Proofs regarding convergence analysis

In this appendix, we display all proofs regarding convergence analysis of BSGD-LMOC.

### Proof of Lemma 1

$$\begin{aligned} s_{k+1} &\leq \frac{k-1}{k} s_k + |\alpha_{n_k}| R \leq \frac{k-1}{k} s_k + \frac{CR}{k} \\ ks_{k+1} &\leq (k-1) s_k + CR \end{aligned}$$

Summing when  $k = 1, \dots, t-1$ , we gain

$$\begin{aligned} (t-1) s_t &\leq (t-1) CR \\ s_t &\leq CR \end{aligned}$$

### Proof of Lemma 2

$$\begin{aligned} \mathbf{w}_t &= \sum_{i \in I_t} \alpha_i \phi(x_i) \\ \|\mathbf{w}_t\| &\leq \sum_{i \in I_t} |\alpha_i| R \leq R s_t \leq CR^2 \end{aligned}$$

### Proof of Lemma 3

$$\begin{aligned} g_t &= \mathbf{w}_t - C \mathbb{I}_{y_{n_t} \mathbf{w}^\top \phi(x_{n_t}) < \theta_{n_t}} y_{n_t} \phi(x_{n_t}) \\ \|g_t\| &\leq \|\mathbf{w}_t\| + CR \leq CR^2 + CR \end{aligned}$$

### Proof of Lemma 4

We assume that the data sample  $\phi(x_{p_t})$  is sampled at  $m$  iterations  $k_1, k_2, \dots, k_m$ . At the iteration  $k_i$ ,  $\phi(x_{p_t})$  arrives in and the correspondent coefficient is added by  $\frac{-Cl'(\mathbf{w}_{k_i}; x_{p_t}, y_{p_t})}{k_i}$  where  $l(\mathbf{w}; x, y) = \max\{0, \theta - y\mathbf{w}^\top \phi(x)\}$  with  $\theta = (1-y)/2$ . At the iteration  $t$ , the above quantity becomes

$$\frac{t-1}{t} \times \frac{t-2}{t-1} \times \dots \times \frac{k_i}{k_i+1} \times \frac{-Cl'(\mathbf{w}_{k_i}; x_{p_t}, y_{p_t})}{k_i} = \frac{-Cl'(\mathbf{w}_{k_i}; x_{p_t}, y_{p_t})}{t}$$

Therefore, the following is guaranteed

$$|\alpha_{p_t}| \leq \sum_{i=1}^m \left\| \frac{Cl'(\mathbf{w}_{k_i}; x_{p_t}, y_{p_t})}{t} \right\| \leq \frac{mCR}{t}$$

### Proof of Lemma 5

$$\|h_t\| \leq |\rho_{p_t}| \|\phi(x_{p_t})\| = t |\alpha_{p_t}| \|\phi(x_{p_t})\| \leq mCR^2 = H$$

### Proof of Lemma 6

$$\begin{aligned} \|\mathbf{w}_{t+1} - \mathbf{w}^*\|^2 &= \|\mathbf{w}_t - \eta_t g_t - Z_t \alpha_{p_t} \phi(x_{p_t}) - \mathbf{w}^*\|^2 = \|\mathbf{w}_t - \eta_t g_t - \eta_t h_t - \mathbf{w}^*\|^2 \\ &= \|\mathbf{w}_t - \mathbf{w}^*\|^2 + \eta_t^2 \|g_t + h_t\|^2 - 2\eta_t (\mathbf{w}_t - \mathbf{w}^*)^\top g_t - 2\eta_t (\mathbf{w}_t - \mathbf{w}^*)^\top h_t \end{aligned}$$

Taking the conditional expectation w.r.t  $\mathbf{w}_t$ , we gain

$$\begin{aligned}
\mathbb{E} \left[ \|\mathbf{w}_{t+1} - \mathbf{w}^*\|^2 \right] &\leq \mathbb{E} \left[ \|\mathbf{w}_t - \mathbf{w}^*\|^2 \right] + \eta_t^2 (G + H)^2 \\
&\quad - 2\eta_t (\mathbf{w}_t - \mathbf{w}^*)^\top \mathbb{E} [g_t] - 2\eta_t (\mathbf{w}_t - \mathbf{w}^*)^\top \mathbb{E} [h_t] \\
&\leq \mathbb{E} \left[ \|\mathbf{w}_t - \mathbf{w}^*\|^2 \right] + \eta_t^2 (G + H)^2 \\
&\quad - 2\eta_t (\mathbf{w}_t - \mathbf{w}^*)^\top \mathcal{J}'(\mathbf{w}_t) - 2\eta_t (\mathbf{w}_t - \mathbf{w}^*)^\top \mathbb{E} [h_t] \\
&\leq \mathbb{E} \left[ \|\mathbf{w}_t - \mathbf{w}^*\|^2 \right] + \eta_t^2 (G + H)^2 \\
&\quad - \frac{2\eta_t \|\mathbf{w}_t - \mathbf{w}^*\|^2}{2} - 2\eta_t (\mathbf{w}_t - \mathbf{w}^*)^\top \mathbb{E} [h_t]
\end{aligned}$$

Here we note that we have used the following inequality

$$(\mathbf{w}_t - \mathbf{w}^*)^\top \mathcal{J}'(\mathbf{w}_t) \geq \mathcal{J}(\mathbf{w}_t) - \mathcal{J}(\mathbf{w}^*) + \frac{1}{2} \|\mathbf{w}_t - \mathbf{w}^*\|^2 \geq \frac{1}{2} \|\mathbf{w}_t - \mathbf{w}^*\|^2$$

Taking the expectation again, we achieve

$$\begin{aligned}
\mathbb{E} \left[ \|\mathbf{w}_{t+1} - \mathbf{w}^*\|^2 \right] &\leq \frac{t-1}{t} \mathbb{E} \left[ \|\mathbf{w}_t - \mathbf{w}^*\|^2 \right] + \eta_t^2 (G + H)^2 - 2\eta_t \mathbb{E} \left[ (\mathbf{w}_t - \mathbf{w}^*)^\top h_t \right] \\
&\leq \frac{t-1}{t} \mathbb{E} \left[ \|\mathbf{w}_t - \mathbf{w}^*\|^2 \right] + \eta_t^2 (G + H)^2 \\
&\quad + 2\eta_t \mathbb{E} \left[ \|\mathbf{w}_t - \mathbf{w}^*\|^2 \right]^{1/2} \mathbb{E} \left[ \|h_t\|^2 \right]^{1/2} \\
&\leq \frac{t-1}{t} \mathbb{E} \left[ \|\mathbf{w}_t - \mathbf{w}^*\|^2 \right] + \frac{(G + H)^2}{t} + \frac{2H \mathbb{E} \left[ \|\mathbf{w}_t - \mathbf{w}^*\|^2 \right]^{1/2}}{t}
\end{aligned}$$

Choosing  $W = H + \sqrt{H^2 + (G + H)^2}$ , we have the following: if  $\mathbb{E} \left[ \|\mathbf{w}_t - \mathbf{w}^*\|^2 \right] \leq W^2$ ,  $\mathbb{E} \left[ \|\mathbf{w}_{t+1} - \mathbf{w}^*\|^2 \right] \leq W^2$ .

**Proof of Theorem 7**

$$\begin{aligned}
\|\mathbf{w}_{t+1} - \mathbf{w}^*\|^2 &= \|\mathbf{w}_t - \eta_t g_t - Z_t \alpha_{p_t} \phi(x_{p_t}) - \mathbf{w}^*\|^2 = \|\mathbf{w}_t - \eta_t g_t - \eta_t h_t - \mathbf{w}^*\|^2 \\
&= \|\mathbf{w}_t - \mathbf{w}^*\|^2 + \eta_t^2 \|g_t + h_t\|^2 - 2\eta_t (\mathbf{w}_t - \mathbf{w}^*)^\top g_t - 2\eta_t (\mathbf{w}_t - \mathbf{w}^*)^\top h_t \\
(\mathbf{w}_t - \mathbf{w}^*)^\top g_t &= \frac{\|\mathbf{w}_t - \mathbf{w}^*\|^2 - \|\mathbf{w}_{t+1} - \mathbf{w}^*\|^2}{2\eta_t} + \frac{\eta_t \|g_t + h_t\|^2}{2} - (\mathbf{w}_t - \mathbf{w}^*)^\top h_t \\
&= \frac{\|\mathbf{w}_t - \mathbf{w}^*\|^2 - \|\mathbf{w}_{t+1} - \mathbf{w}^*\|^2}{2\eta_t} + \frac{\eta_t \|g_t + h_t\|^2}{2} - (\mathbf{w}_t - \mathbf{w}^*)^\top Z_t \rho_{p_t} \phi(x_{p_t})
\end{aligned}$$

Taking the conditional expectation w.r.t  $\mathbf{w}_1, \dots, \mathbf{w}_t, x_1, \dots, x_t$  of two sides on

the above inequality, we gain

$$\begin{aligned}
(\mathbf{w}_t - \mathbf{w}^*)^\top \mathcal{J}'(\mathbf{w}_t) &\leq \frac{\mathbb{E}[\|\mathbf{w}_t - \mathbf{w}^*\|^2] - \mathbb{E}[\|\mathbf{w}_{t+1} - \mathbf{w}^*\|^2]}{2\eta_t} \\
&\quad + \frac{\eta_t(G+H)^2}{2} - (\mathbf{w}_t - \mathbf{w}^*)^\top \mathbb{E}[Z_t] \rho_{p_t} \phi(x_{p_t}) \\
\mathcal{J}(\mathbf{w}_t) - \mathcal{J}(\mathbf{w}^*) + \frac{1}{2} \|\mathbf{w}_t - \mathbf{w}^*\|^2 &\leq \frac{\mathbb{E}[\|\mathbf{w}_t - \mathbf{w}^*\|^2] - \mathbb{E}[\|\mathbf{w}_{t+1} - \mathbf{w}^*\|^2]}{2\eta_t} \\
&\quad + \frac{\eta_t(G+H)^2}{2} - \mathbb{P}(Z_t = 1) \rho_{p_t} (\mathbf{w}_t - \mathbf{w}^*)^\top \phi(x_{p_t})
\end{aligned}$$

Here we note that  $\rho_{p_t}$  is functionally dependent on  $\mathbf{w}_1, \dots, \mathbf{w}_t, x_1, \dots, x_t$  and  $\mathcal{J}(\mathbf{w})$  is 1-strongly convex function.

Taking the expectation of two sides of the above inequality, we obtain

$$\begin{aligned}
\mathbb{E}[\mathcal{J}(\mathbf{w}_t) - \mathcal{J}(\mathbf{w}^*)] &\leq \frac{t-1}{2} \mathbb{E}[\|\mathbf{w}_t - \mathbf{w}^*\|^2] - \frac{t}{2} \mathbb{E}[\|\mathbf{w}_{t+1} - \mathbf{w}^*\|^2] \\
&\quad + \frac{(G+H)^2}{2t} - \mathbb{P}(Z_t = 1) \mathbb{E}[(\mathbf{w}_t - \mathbf{w}^*)^\top \rho_{p_t} \phi(x_{p_t})] \\
\mathbb{E}[\mathcal{J}(\mathbf{w}_t) - \mathcal{J}(\mathbf{w}^*)] &\leq \frac{t-1}{2} \mathbb{E}[\|\mathbf{w}_t - \mathbf{w}^*\|^2] - \frac{t}{2} \mathbb{E}[\|\mathbf{w}_{t+1} - \mathbf{w}^*\|^2] + \frac{(G+H)^2}{2t} \\
&\quad + \mathbb{P}(Z_t = 1) \mathbb{E}[\|\mathbf{w}_t - \mathbf{w}^*\|^2]^{1/2} \mathbb{E}[\|\rho_{p_t} \phi(x_{p_t})\|^2]^{1/2} \\
&\leq \frac{t-1}{2} \mathbb{E}[\|\mathbf{w}_t - \mathbf{w}^*\|^2] - \frac{t}{2} \mathbb{E}[\|\mathbf{w}_{t+1} - \mathbf{w}^*\|^2] \\
&\quad + \frac{(G+H)^2}{2t} + \mathbb{P}(Z_t = 1) RW \mathbb{E}[\rho_{p_t}^2]^{1/2}
\end{aligned}$$

Taking sum when  $t = 1, \dots, T$ , we gain

$$\begin{aligned}
\sum_{t=1}^T \mathbb{E}[\mathcal{J}(\mathbf{w}_t) - \mathcal{J}(\mathbf{w}^*)] &\leq \frac{(G+H)^2}{2} \sum_{t=1}^T \frac{1}{t} + RW \sum_{t=1}^T \mathbb{P}(Z_t = 1) \mathbb{E}[\rho_{p_t}^2]^{1/2} \\
\frac{1}{T} \sum_{t=1}^T \mathbb{E}[\mathcal{J}(\mathbf{w}_t)] - \mathcal{J}(\mathbf{w}^*) &\leq \frac{(G+H)^2 (\log T + 1)}{2T} + \frac{WR}{T} \sum_{t=1}^T \mathbb{P}(Z_t = 1) \mathbb{E}[\rho_{p_t}^2]^{1/2} \\
\mathbb{E}[\mathcal{J}(\bar{\mathbf{w}}_t)] - \mathcal{J}(\mathbf{w}^*) &\leq \frac{1}{T} \sum_{t=1}^T \mathbb{E}[\mathcal{J}(\mathbf{w}_t)] - \mathcal{J}(\mathbf{w}^*) \leq \frac{(G+H)^2 (\log T + 1)}{2T} \\
&\quad + \frac{WR}{T} \sum_{t=1}^T \mathbb{P}(Z_t = 1) \mathbb{E}[\rho_{p_t}^2]^{1/2}
\end{aligned}$$